Polar Biol (2008) 31:617–628
DOI 10.1007/s00300-007-0398-4

ORIGINAL PAPER

In situ and remote-sensed chlorophyll fluorescence as indicator of the physiological state of phytoplankton near the Isles Kerguelen (Southern Ocean)

Klaas R. Timmermans · Hendrik J. van der Woerd · Marcel R. Wernand · Merijn Sligting · Julia Uitz · Hein J. W. de Baar

Received: 20 April 2007 / Revised: 23 November 2007 / Accepted: 26 November 2007 / Published online: 10 January 2008

Abstract Shipboard and remote-sensed Chlorophyll fluorescence were determined in the natural phytoplankton assemblage above the iron-enriched Kerguelen Plateau and the adjacent high-nutrient, low-Chlorophyll open Southern Ocean. The variance between fluorescence yield and photosynthetic efficiency was determined in combination with Chlorophyll *a* concentrations, irradiance and phytoplankton species distribution. A co-variance between the fluorescence measurements would allow the refinement of remote-sensing primary production algorithms. Distinct differences were found in photosynthetic efficiency and water-leaving fluorescence, with relatively high values for the Kerguelen Plateau and low values in the open ocean, reflecting the differences in Chlorophyll *a* concentrations. The co-variance of the fluorescence properties suggested that remote-sensed fluorescence measurements could be used to infer differences in the physiological state of the phytoplankton, hence primary production. Fluorescence yield, however, did not show the differences in the research area, most likely due to the low signal and the diurnal variation in water-leaving fluorescence.

K. R. Timmermans (✉) · M. R. Wernand · M. Sligting · H. J. W. de Baar
Royal Netherlands Institute for Sea Research (NIOZ),
P.O. Box 59, 1790 AB Den Burg, Texel, The Netherlands
e-mail: klaas@nioz.nl

H. J. van der Woerd · M. Sligting
Institute for Environmental Studies, Vrije Universiteit,
De Boelelaan 1087, 1081 HV Amsterdam, The Netherlands

J. Uitz
Laboratoire d'Oceanographie de Villefranche,
CNRS and Universite Pierre et Marie Curie, Quai de la Darse,
BP 08, 06 238 Villefranche-sur-Mer Cedex, France

Keywords Phytoplankton · Fluorescence · Remote sensing · Photosynthetic efficiency · Fluorescence yield · Southern Ocean

Introduction

Satellite observations have proven to be of great use for estimating the worldwide oceanic primary production (Behrenfeld and Falkowski 1997; O'Reilly et al. 1998). Satellite-derived primary production is commonly related to the Chlorophyll *a* (Chl *a*) concentration. However, two problems are obvious when using Chl *a* concentration as an indicator for primary production. First, the relation between Chl *a* concentration and phytoplankton biomass is not conservative as a result of the following: (a) the ratio Chl *a* to carbon is species-specific, (b) senescent cells have less pigments than young cells, and (c) light intensity and spectral quality, as well as (micro-)nutrient availability, affect the pigment composition and concentration. Second, the phytoplankton biomass alone does not tell us at which rate the phytoplankton grows. The growth rate of phytoplankton in natural waters differs in response to the environmental conditions and the physiological state of the phytoplankton. An additional problem in polar regions, concerning the remote sensing of Chl *a*, is that the common algorithms used to calculate chlorophyll concentrations from remotely sensed blue–green bands, were found to be inaccurate. The absorptive properties of the phytoplankton in polar waters differed from the absorptive properties of the more temperate waters, to which the algorithms are basically tuned (Mitchell 1992; Dierssen and Smith 2000; Stramska et al. 2003). The pigment-specific absorption was found to be significantly smaller, particularly in the blue region of the spectrum, which was hypothesized to be due

to pigment-packaging effects and a relatively small amount of detrital absorption compared to phytoplankton absorption in polar waters (Mitchell 1992). The magnitude of the inaccuracy differed (Dierssen and Smith 2000; Mitchell 1992; Stramska et al. 2003; Stramska et al. 2006) and seemed to be related to the species composition (Stramska et al. 2003) and the season (Stramska et al. 2006).

Chlorophyll fluorescence, as introduced by Lorenzen (1966), is commonly used as an indicator for phytoplankton biomass, despite the poor relationship between the Chl *a* concentration and the amount of fluorescence emitted. The amount of fluorescence emitted is, besides on the Chl *a* concentration, dependent on the photosynthetic available radiation (PAR), the absorptive properties of the phytoplankton, the extent to which the emitted fluorescence is reabsorbed, and the fluorescence yield (Babin et al. 1996), defined as the fraction of light absorbed by phytoplankton (per unit of Chl *a*) that is re-emitted as fluorescence. The other fraction of the absorbed light is used for photosynthesis (photochemical quenching) or is lost as heat (non-photochemical quenching). Generally speaking, the more efficiently the phytoplankton utilizes the absorbed light for photosynthesis, the less of the absorbed light is re-emitted as fluorescence. Fluorescence, when normalized to PAR, is found to predict Chl *a* concentrations with an accuracy of up to 80% under local conditions (Lorenzen 1966; Kiefer et al. 1989; Chamberlin et al. 1990), but the overall accuracy is found to be about 50% (Parsons et al. 1984). At low Chl *a* concentrations (<2 μg l^{-1}) the relation between Chl *a* and fluorescence at a certain PAR intensity is almost linear (Babin et al. 1996; Gower et al. 2004), but the amount of fluorescence per unit Chl *a* per unit PAR varied between phytoplankton species, is dependent on the current physiological status of the phytoplankton (e.g. affected by (micro-)nutrient availability), and is influenced by the intensity of the solar radiation (Falkowski and Kolber 1995). When the photosynthetic reaction centres of PhotoSystem II (PS II) close in high light, the fluorescence will rise because these closed centres do not quench the fluorescence. Hence, the higher the incident PAR intensity, the more light is re-emitted as fluorescence. In addition: the faster the phytoplankton is able to process absorbed light in the PS II, the less of the absorbed light is re-emitted as fluorescence.

Environmental conditions not only affect the fluorescence yield, but also the photosynthetic efficiency or quantum efficiency of PS II, measured as F_v/F_m using variable fluorescence (Kolber et al. 1988; Behrenfeld and Kolber 1999). For example, photosynthetic efficiency was shown to be a sensitive diagnostic for iron (Fe) limitation of Southern Ocean phytoplankton (Behrenfeld and Kolber 1999; Holeton et al. 2005; Veldhuis and Timmermans 2007). The link between fluorescence yield and photosynthetic efficiency is not straightforward because non-photochemical processes also play a role. The rate of non-photochemical quenching is variable and primarily depending on the incident light conditions. Especially in surface waters, where light intensities are high, non-photochemical processes might influence both the photosynthetic efficiency and the fluorescence yield. Therefore, high-fluorescence values can be caused by both high-phytoplankton biomass with a high-photosynthetic efficiency or low biomass with a low-photosynthetic efficiency. To interpret fluorescence values correctly, and to distinguish between biomass and photosynthetic efficiency, fluorescence values should be compared with Chl *a* concentrations, PAR data, information on the physiological state (e.g. nutrient stress as indicated by active fluorescence measurements) and the species composition of the phytoplankton.

The Southern Ocean contains the largest high-nutrient low-chlorophyll (HNLC) region in the world's oceans, where the major nutrients (nitrate, orthophosphate and silicic acid) are plentiful, but phytoplankton growth is limited by Fe and light (Martin et al. 1990; de Baar et al. 1995). However, both increased Chl *a* concentrations and primary production are occasionally observed, for example at the Polar Front (de Baar et al. 1995), around islands and Plateaus (Blain et al. 2001, 2007; Bucciarelli et al. 2001) or close to melting icebergs and packice (Sedwick and DiTullio 1997). The Kerguelen Plateau typically has been described as such site where increased dissolved Fe concentrations induce phytoplankton blooms (Blain et al. 2001, 2007; Bucciarelli et al. 2001), mainly of the larger-sized diatom species. The Kerguelen region is regarded as a natural laboratory (i.e. stabile but contrasting conditions over a short distance, Blain et al. 2007), with good opportunities to study the effects of natural Fe enrichment in a HNLC region.

During the KEOPS expedition (KErguelen: Ocean and Plateau compared Study) in January-February 2005, the effects of the natural Fe fertilization above the Kerguelen Plateau were studied from a broad perspective (Deep Sea Research: special issue 2008). In this paper, phytoplankton fluorescence as measured at the sea surface with shipboard radiance sensors and in situ passive and active fluorescence measurements on discrete samples, were used to investigate the physiological differences between phytoplankton in the surface waters above the Kerguelen Plateau and in the adjacent open HNLC ocean. The main aim was to link variations in the amount of fluorescence emitted per unit chlorophyll (i.e. fluorescence yield) to differences in photosynthetic efficiency (i.e. F_v/F_m). The second goal was to investigate to which extent satellite remotely sensed parameters, similar to the parameters measured on board, could be used to investigate the photosynthetic efficiency

in a Southern Ocean location. Knowledge on the co-variance between these fluorescence measurements would allow the refinement of remote sensing primary production algorithms.

Materials and methods

The study area was southeast of the Isles Kerguelen in the Southern Ocean, between −48.5° and −53.5° latitude and 68° and 79° longitude (Fig. 1a) and comprised the Fe and phytoplankton-enriched Kerguelen Plateau waters and the adjacent HNLC open ocean. Field campaigns and experiments have given insights into the concentration of (dissolved) Fe and the phytoplankton community in the water column above the Kerguelen Plateau (Blain et al. 2001, 2007; Bucciarelli et al. 2001). Moreover, MODIS satellite data provided an overview of the spatial and temporal variability of phytoplankton bloom events. For the present study, satellite data from December 2004 till February 2005 were analysed (see below). During the KEOPS cruise (19 January–13 February 2005) aboard R.V. Marion Dufresne, the effects of natural Fe fertilisation of the oceanic water of the Kerguelen Plateau on the

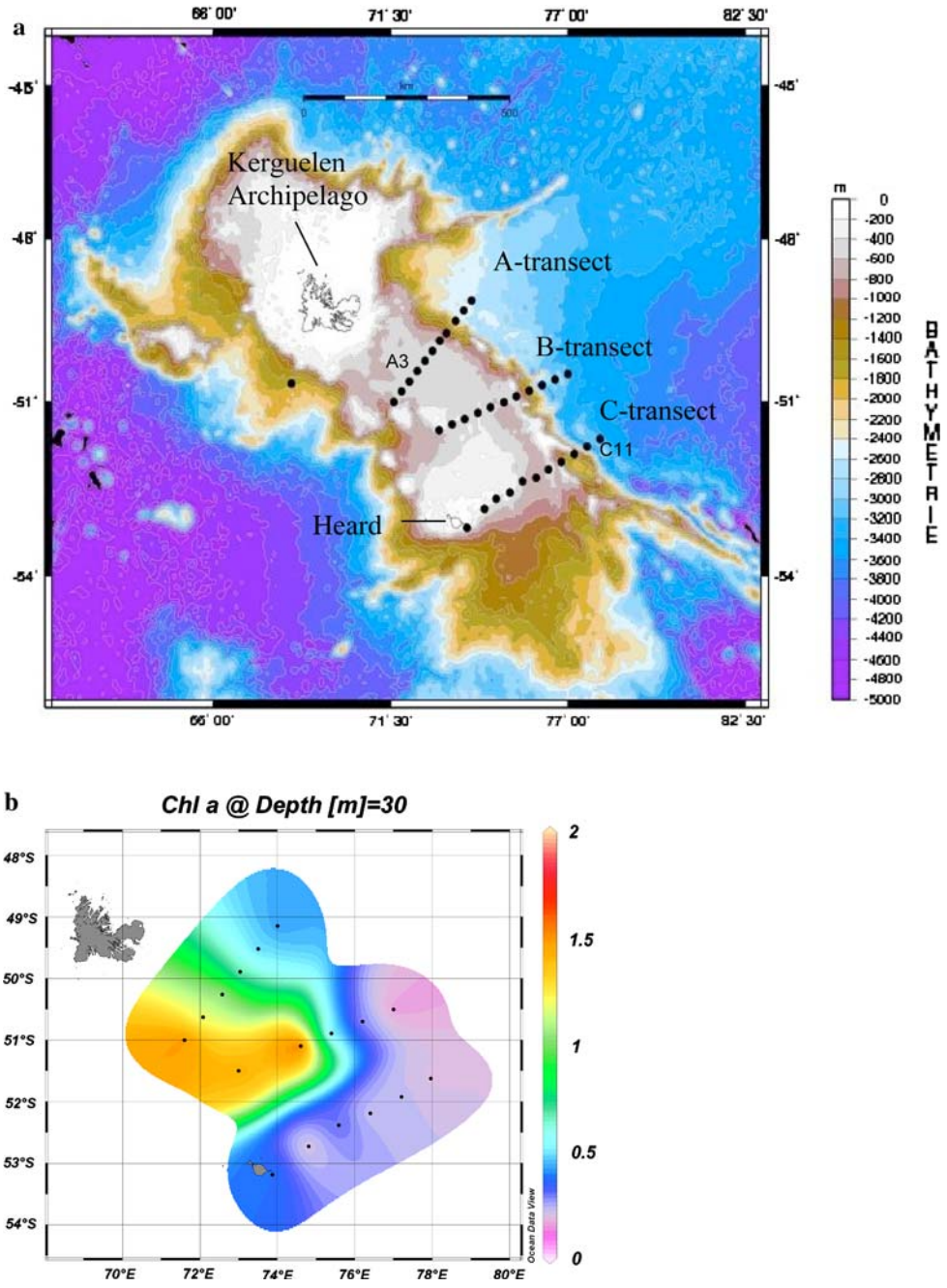

Fig. 1 **a** KEOPS research area with A, B, and C transects. Above the Kerguelen Plateau average water depth was about 500 m, at the open ocean more than 2,000 m. Main sampling stations A3 and C11 are indicated. **b** Chl *a* (μg l^{-1}) distribution at 30 m depth. Chl *a* concentrations <0.5 μg l^{-1} were defined as open ocean conditions, Chl *a* concentrations >0.5 μg l^{-1} were defined as Plateau bloom conditions

biological pump and the cycling of other chemical compounds relevant for climate change were studied and compared to the adjacent open Southern Ocean (Blain et al. 2007). The study area was sampled over three transects; the cruise stations were divided over the Chl *a* gradient from the open Southern Ocean towards the Kerguelen Plateau (Fig. 1a, b). Especially station A3 (position 50°38 S, 72°05 E) situated above the Kerguelen Plateau, and open ocean surface water (HNLC) sampling station C11 (position 51°39 S, 78°00 E) were sampled several times and served as example stations for the Plateau versus the open ocean, respectively. With a few exceptions, most other stations were sampled once. A full overview of the parameters investigated during the KEOPS cruise can be found at: http://www.obsvlfr.fr.proof/vt/op/ec/keops/keo.htm

Using discrete samples, F_0 (Chl *a* autofluorescence) and the photosynthetic efficiency, F_v/F_m (variable fluorescence F_v over maximum fluorescence F_m, where $F_v = F_m - F_0$) were measured using Pulse Amplitude Modulated (PAM) fluorometry (PHYTOPAM, Walz, Germany) on freshly collected, dark-adapted samples from the upper 200 m of the water column (Schreiber et al. 1993; Kromkamp and Forster 2003). Because the phytoplankton was dominated by diatoms, we used the data obtained with the PHYTO-PAM blue light as these gave the strongest fluorescence signals. The results for the other measuring light colours did not differ however, suggesting that cyanobacteria were a negligible fraction of the population. The latter was confirmed by flow cytometer analyses and microscope observations (Timmermans et al. 2008; Armand et al. 2008). The samples were dark-adapted for 20–40 min including the time spent on the NISKIN bottles during sampling before the PHYTOPAM measurements were made. Filtered seawater (Sartorius Sartobran, 0.2 μm) was used for blank measurements.

Two RAMSES ARC hyper-spectral radiance sensors (field of view of 7° in air) were positioned on the top of the bridge of the R.V. Marion Dufresne and looked at a nadir angle of 35° to the water surface to measure the upwelling radiance above the sea surface (L_{sfc}). Because of the high seas in the Southern Ocean, accurate measurements of the incident sky radiance (e.g. Mobley 1999) at exactly the right angle were difficult to obtain from a fixed position on the bridge. Therefore we decided to place the two sensors 90° apart in the horizontal plane (one at starboard, the other at port side) to avoid sun glint and apply an approximate correction for specular reflection of sky radiance, based on irradiance measurements. An additional RAMSES ACC radiometer (cosine) was mounted in the mast to measure the incident solar irradiance E_S. PAR was calculated from the sum of $E_s(\lambda)$ between the wavelengths (λ) 400 and 700 nm. The optical sensors were manufactured by TriOS Mess- und Datentechnik GmbH, Germany (Heuermann et al. 1999), and in this paper fluorescence data derived from above-water spectra are indicated as TRIOS–FLH. The spectral range of the radiometers was between 350 and 1,000 nm over a maximum of 200 channels. Measurements were taken over the whole spectral range every 3.2 nm. Spectra were collected every 15 min. An automatic quality control procedure was applied to check for precipitation and for minimal solar incoming radiation level, dusk and dawn conditions (red colouring of the sky). From each duplo of above-water radiance spectra, the spectrum with the least sky glint contamination was selected, according to Wernand (2002). As no measurements were made of the sky radiance (L_{sky}), it was assumed that any above-water radiance measured near 940 nm could be attributed to specular reflection of skylight. From the simultaneously measured radiance spectra (L_{sfc}) and irradiance spectra E_s the fraction F at 940 nm was calculated,

$$F_{940} = \frac{L_{sfc940}}{E_{S940}} \quad (1)$$

Subsequently all L_{sfc} were spectrally corrected for sky radiance by subtracting the product $F_{940}{}^*E_s$, in order to the derive the quasi water-leaving radiance $L_{qw}(\lambda)$ given by

$$L_{qw}(\lambda) = L_{sfc}(\lambda) - F_{940} * E_S(\lambda) \quad (2)$$

In the further analysis of the spectra it was found that the FLH method was not very sensitive to the value of F_{940}. This was mainly due to the robustness of the baseline method and choice of the reference wavelengths (Letelier and Abbott 1996).

The MODIS sensor on the AQUA satellite provided images with a spatial resolution of typically 1 km in 9 spectral bands between 400 and 900 nm. Spectral bands in the blue–green part of the spectrum (e.g. MODIS at 443 and 551 nm) allowed calculation of Chl *a* concentrations (OC3 algorithm)(O'Reilly et al. 1998). MODIS bands 13, 14 and 15 (centred at 665.5, 676.8 and 746.4 nm, respectively) were used to assess the fluorescence (MODIS–FLH) emitted by Chl *a*. The time of image acquisition varied between 9.05 and 9.55 h local time. Most images of the Kerguelen region had cloud cover close to 90% or more. The satellite data were downloaded from the NASA ocean colour site (http://www.oceancolor.gsfc.nasa.gov/) and was processed by the SeaDAS software (Version 4.7). The Chl *a* and FLH products were taken from a grid of 5 × 5 pixels centred at the stations sampled at sea. The data were kept for analysis only if no pixels were masked as clouds and if large spatial variation in the products was absent. The existence of large gradients over 5 pixels (approximately 5 km) was therefore used as an indication of incorrect recognition of clouds or other atmospheric disturbances. From the 65 overpasses in December 2004, January and February 2005, around 4.30 UTC or 9.30 h local time, 16

images contained measurements of the stations sampled at sea. However, matches in time, where a satellite-derived value matched within one hour with a value measured on board, did not occur.

Seawater samples for HPLC-determined Chl *a* were collected from NISKIN bottles attached to a CTD rosette frame at 10, 20, 30 and 40 m depth (hereafter indicated as surface waters). Samples were filtered through 25-mm Whatman GF/F glass-fiber filters with a nominal pore size of 0.7 μm. Filtration volumes varied between 1.5 and 2.8 l for the bloom region and the HNLC waters, respectively. Filters were placed into cryotubes, frozen, and stored in liquid nitrogen until laboratory analysis. Pigment extraction and analysis were carried out in the laboratory following a method derived from that of Van Heukelem and Thomas (2001) and comprehensively described in Ras et al. (submitted). Essentially, samples were extracted at −20°C in 3 ml methanol (100%) for 1-h minimum. The extracts were clarified by vacuum filtration through Whatman GF/F filters, and injected onto a reversed-phase C8 Zorbax Eclipse column (dimension: 3 × 150 mm, 3.5 μm pore size). Instrumentation comprised an Agilent Technologies 1100 series HPLC system, equipped with diode array detection at 450, 667 and 770 nm. Ultimately, the number of HPLC Chl *a* analyses determined the number of comparisons that could be made between active and passive fluorescence using the PHYTOPAM. Cloudcover and mismatch between in situ sampling and satellite overpasses further limited the comparison of in situ and remote-sensed measurements. Stations A3 (Plateau) and C11 (open Southern Ocean) were sampled most frequently, but results are presented whenever there was a match between the parameters.

Solar-induced fluorescence in case-I waters resulted in a weak but detectable signal in the water-leaving radiance near 685 nm. In the Kerguelen region the fluorescence only contributed in the order of a few percent to the signal near 685 nm, and special care was taken to retrieve this weak signal. We followed the pioneering work of Neville and Gower (1977) and Gower (1980), who investigated the potential of the relatively simple FLH method to measure fluorescence intensity. This FLH method relies on three independent measurements: one near the maximum of Chl *a* fluorescence emission (683–685 nm) and two readings (665 and 746 nm) to define a 'baseline' below the fluorescence peak. The FLH derived from the TRIOS sensors above-water radiance measurements was calculated as:

$$\begin{aligned}\text{TRIOS} - \text{FLH} = {} & L_{\text{qw}}(\lambda_{677}) - kL_{\text{qw}}(\lambda_{665}) \\ & - (1-k)L_{\text{qw}}(\lambda_{746}) \end{aligned} \quad (3)$$

where L_{qw} is the radiance of waveband λ calculated according to Eq. 2 and k is a factor $((746 - 677)/(746 - 665) \approx 0.85)$ that corrects for the position of λ_2 relative to λ_1 and λ_3 (Abbott and Letelier 1999). To enable a comparison between the shipboard and the satellite-mounted radiometers we took the three wavelength positions identical to the mean positions of the MODIS fluorescence bands 13, 14 and 15, respectively, 664.6, 676.7 and 746.3 nm. It should be noted that MODIS band 14 is well off the wavelength of maximum emission of fluorescence (685 nm) and very close to the in situ red absorption maximum of Chl *a*. So the negative and variable atmospheric influence due to oxygen absorption lines, which is high at 687 nm, could be avoided. The exact procedures and scientific background on the computation of MODIS–FLH can be found in the algorithm theoretical basis documents (Abbott and Letelier 1999). Note that because of the particular band setting of MODIS the detected FLH is estimated to be between 0.6 (Gower et al. 2004) and 0.7 (Huot et al. 2005) of the actual emission maximum at 685 nm. Due to the positioning of band 15, at more than 60 nm from the fluorescence emission maximum, the baseline is slightly overestimated at small Chl *a* concentrations, which results in negative FLH values (Letelier and Abbott 1996). It is important to realize that the attenuation by water in the 685-nm wavelength region is large, such that the depth from which 90% of the fluorescence signal originates is only the upper 4 m of the sea (Eq. 29 in Babin et al. 1996). Letelier and Abbott (1996) compared the FLH with the expected signal to noise of the MODIS satellite. Their work suggested a detection limit of MODIS–FLH of about 0.012 mW m^{-2} sr^{-1} μm^{-1}, corresponding to a mean value of 0.3 μg Chl *a* l^{-1}.

Results

The surface water HPLC Chl *a* concentrations in the Kerguelen study area ranged between 0.11 μg l^{-1} at open ocean station C11 to 1.45 μg l^{-1} at Plateau bloom station A3 (Figs. 1b, 2, 3). We defined Plateau stations by Chl *a* concentrations >0.5 μg l^{-1}, and open ocean stations by Chl *a* concentrations <0.5 μg l^{-1}. The passive (F_0) and active (F_v/F_m) fluorescence measurements (PHYTOPAM) revealed similar differences between Plateau and open ocean stations. F_0 in surface waters varied between 11, typical for the HNLC open ocean stations, and about 1,000, at bloom station A3 (Fig. 2). This resulted in a positive correlation between F_0 values and Chl *a* concentrations, with a R^2 of 0.71 (Fig. 2). Over the Plateau, the F_v/F_m values ranged from about 0.4 to 0.6, whereas in the open ocean the F_v/F_m values varied between 0.2 and 0.4 (Fig. 3a). In principle, F_v/F_m is not dependent on the biomass present. Nevertheless, we observed that the F_v/F_m values correlated positively with the HPLC Chl *a* concentrations (Fig. 3a). The R^2 of the correlation was 0.53. Most likely, the low Fe availability in the open ocean caused both low growth rates and a low photosynthetic

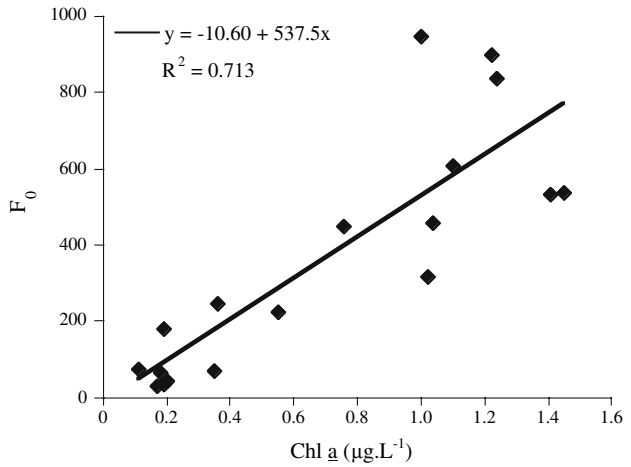

Fig. 2 Chl *a* autofluorescence (PHYTOPAM, F_0 in blue light) against HPLC Chl *a* concentrations (µg l^{-1}) in surface water samples from the KEOPS research area

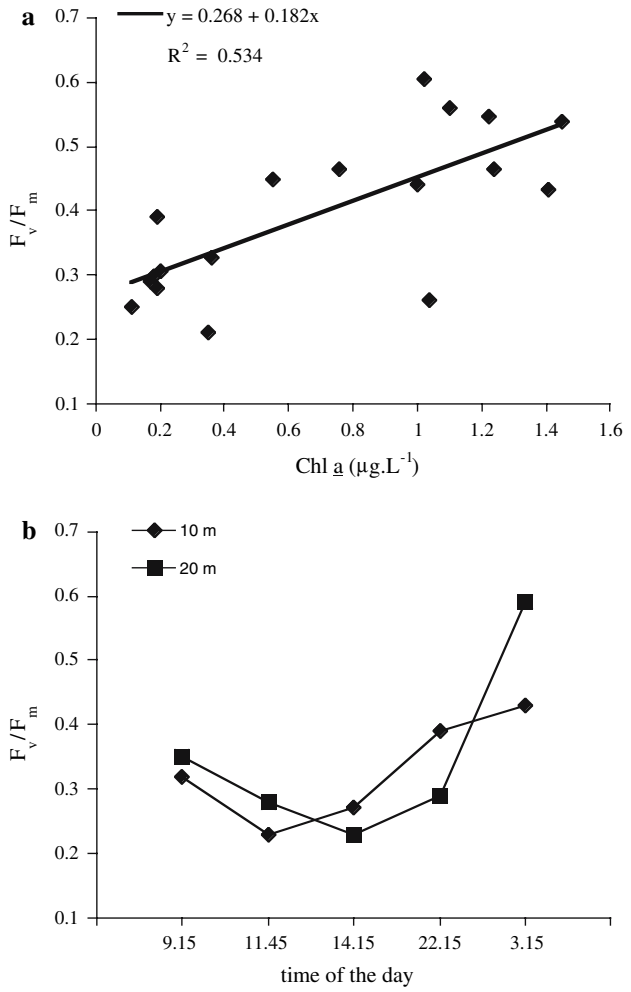

Fig. 3 **a** Photosynthetic efficiency (F_v/F_m) against HPLC Chl *a* concentrations (µg l^{-1}). **b** F_v/F_m during the day (11–12 February 2005) at Plateau bloom station A3, sampled at 9.15, 11.45, 14.15, 22.15 and 3.15 h (local time) at 10 and 20 m depth

efficiency, whereas above the Plateau both were enhanced. Obviously, the phytoplankton above the Plateau was in a better physiological condition than the phytoplankton in the open ocean. The phytoplankton bloom above the Plateau, with high F_v/F_m values, and the low F_v/F_m values at the open ocean, matched well with the findings of Blain et al. (Blain et al. 2007, 2008), who found during the KEOPS cruise a relatively high flux of (bioavailable) Fe to the surface waters above the Kerguelen Plateau and a low Fe flux towards the surface waters of the open ocean. The enhanced natural Fe input from subsurface waters triggered the phytoplankton bloom above the Kerguelen Plateau (Blain et al. 2007). Photosynthetic efficiency appeared not only to be dependent on physiological condition of the phytoplankton, but also varied during the day, with a gradual decline till 12.00 h, after which it increased again (Fig. 3b), and over the depth (no data shown).

The solar-induced fluorescence emitted from the sea surface (TRIOS–FLH), as repeatedly measured with optical sensors mounted at the ship resulted in multiple measurements per station. But many stations were sampled at night or at dusk or dawn, when no reliable optical measurements of the sea surface could be made. Moreover, many of the optical spectra were contaminated with a high amount of reflectance, which was interpreted as an artefact of the high-wave activity and the resulting high amounts of foam on the sea surface during the cruise. The TRIOS–FLH measurements that remained after selection (see Materials and methods), correlated strongly with the surface Chl *a* concentration, with an R^2 of 0.84 (Fig. 4a). The TRIOS–FLH values ranged from 0.015 to 0.093 mW m^{-2} sr^{-1} μm^{-1}. Negative FLH values do not in principle mean that there is no fluorescence. It only indicates that the height of the fluorescence peak lies below the defined base line (Fig. 4b). Nevertheless, the TRIOS–FLH values measured in the cruise area were small and probably hit the detection limit ($\approx$0.012 mW m^{-2} sr^{-1} μm^{-1} for the MODIS satellite sensor, Letelier and Abbott 1996).

The increased Chl *a* concentrations and fluorescence values above the Kerguelen Plateau corresponded with an increased phytoplankton biomass above the Plateau as observed by Armand et al. (2008) during the KEOPS cruise. Armand et al. reported phytoplankton biomass ranging from 2.5 to 25.7 µg C l^{-1} in the open ocean, whereas above the Kerguelen Plateau the phytoplankton biomass varied between 45.6 and 99.4 µg C l^{-1}. The Chl *a* concentrations measured (HPLC) and calculated from satellite data (MODIS) indicated a decline at station A3 (Fig. 5a) during the KEOPS cruise. Also the photosynthetic efficiency (F_v/F_m) decreased at station A3 towards the end of the cruise (Fig. 5b).

Intercomparison of the F_0 and shipboard TRIOS–FLH showed a positive correlation (Fig. 6a, R^2 = 0.77). For

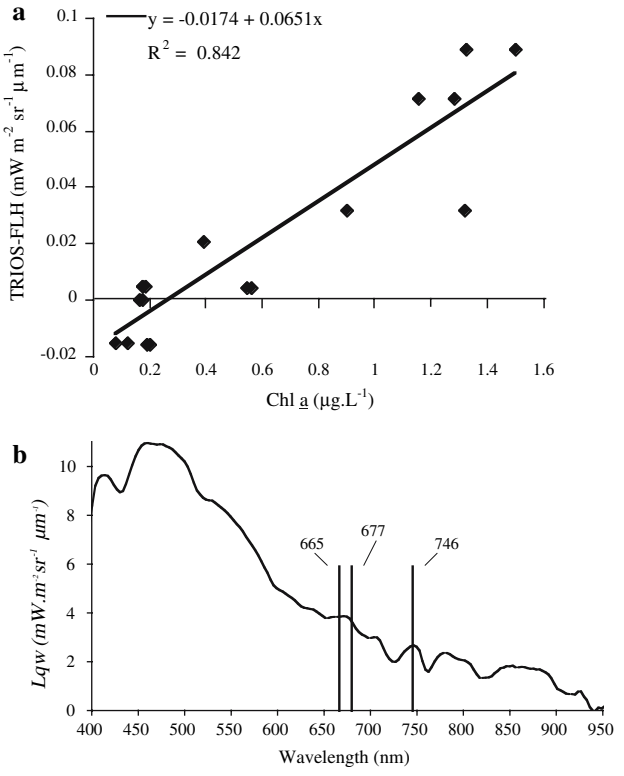

Fig. 4 **a** Shipboard TRIOS–FLH (mW m^{-2} sr^{-1} μm^{-1}) against HPLC Chl *a* concentrations (µg l^{-1}) in surface water samples from the KEOPS research area. **b** Typical example of the L_{qw} spectrum used to calculated FLH according to Eq. (3), calculated for the 2nd of February 2005 at Plateau bloom station A3 with HPLC Chl *a* concentration of 1.1 µg l^{-1}

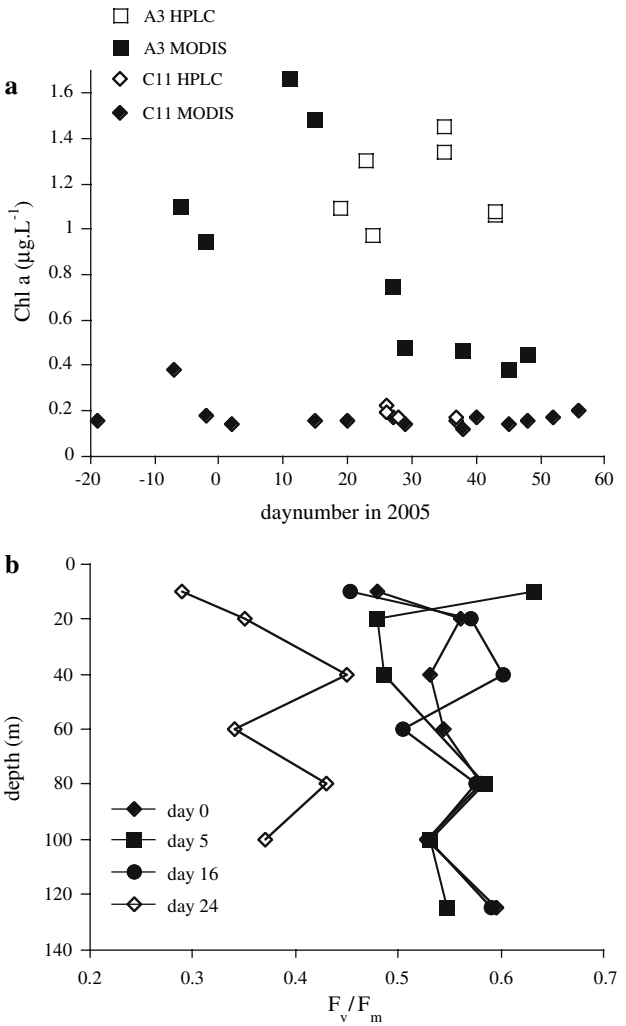

Fig. 5 Evolution during the KEOPS cruise of: **a** MODIS-derived Chl *a* (December 2004, January and February 2005) and in situ surface water HPLC Chl *a* concentrations (both in µg l^{-1}) at Plateau bloom station A3 and open ocean station C11. **b** Photosynthetic efficiency (F_v/F_m) at Plateau bloom station A3 at daylight conditions on day 0, 5, 16 and 24 against depth (m)

photosynthetic efficiency (F_v/F_m) and TRIOS–FLH, the relationship was still present, but weaker than with F_0 (Fig. 6b, R^2 = 0.49). For F_v/F_m and TRIOS–FLH two clusters of data appeared to be present, one smaller than 0.06 and one larger than 0.08 mW m^{-2} sr^{-1} μm^{-1}, typical for open ocean and Kerguelen Plateau conditions, respectively.

Although the difference in photosynthetic efficiency between the Kerguelen Plateau and the adjacent open ocean was obvious (Figs. 2, 3a), the amount of fluorescence (TRIOS–FLH) emitted per unit chlorophyll (fluorescence yield) did not differ between the open ocean (<0.5 µg Chl *a* l^{-1}) and the Plateau (>0.5 µg Chl *a* l^{-1}) (Fig. 7a). The lack of a gradient in the fluorescence yield is also shown in Fig. 7b, where an additional correction for the incident solar light intensity (PAR, integrated between 400 and 700 nm) was applied. An important source of uncertainty in the retrieval of the fluorescence yield estimates was the influence of the daily irradiation cycle on the FLH. In Fig. 8a the TRIOS–FLH, normalized to the in situ measured Chl *a* value was plotted as a function of the local time. The amount of fluorescence emitted per unit chlorophyll seemed to increase during the day, by a factor of about two on average, between 7:00 and 17:00 h. However, when normalized for PAR (Fig. 8b), the fluorescence per unit chlorophyll was relatively high at the beginning and the end of the day, with a profound depression during the middle of the day, similar to the F_v/F_m measurements at Plateau bloom station A3 during the day (Fig. 3b).

No matching within 1 h of the satellite overpass between MODIS–FLH and HPLC Chl *a* or TRIOS–FLH data occurred due to regular heavy cloud cover and because a large part of the in situ sampling took place at night time or dawn or dusk, when no reliable spectroscopic measurements could be obtained. The satellite image (both Chl *a* and FLH) with the least cloud cover, made at the 27th of January 2007, is shown in Fig. 9. The increased Chl *a* concentrations above the Kerguelen Plateau and in eddies east of the Kerguelen Archipelago (Fig. 9a) coincided with increased fluorescence

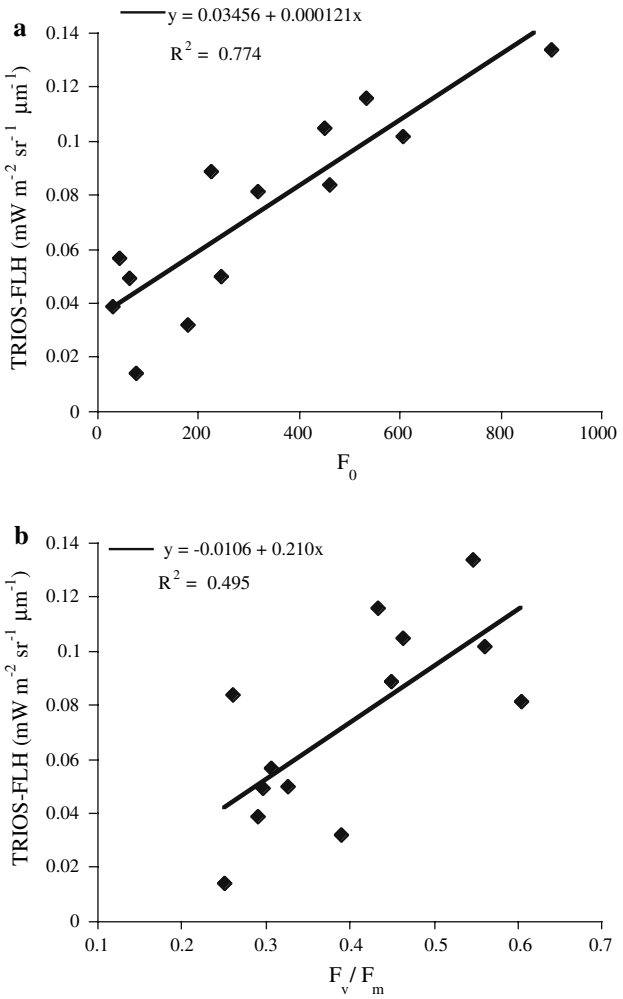

Fig. 6 Intercomparison of TRIOS–FLH and PHYTOPAM measurements in surface water samples from the KEOPS research area: **a** Chl *a* autofluorescence (PHYTOPAM F_0 in blue light) against TRIOS–FLH (mW m^{-2} sr^{-1} μm^{-1}). **b** Photosynthetic efficiency (F_v/F_m,) against TRIOS–FLH (mW.m^{-2} sr^{-1} μm^{-1})

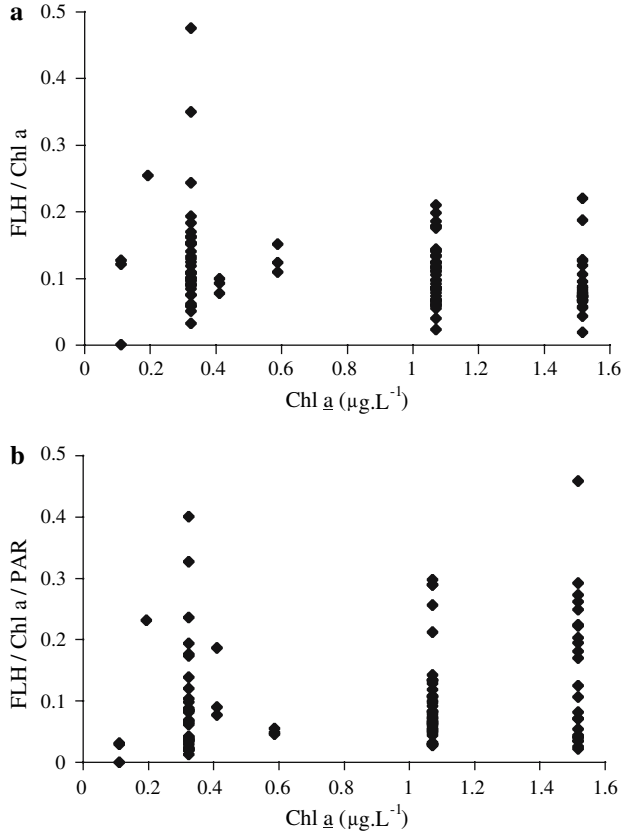

Fig. 7 **a** Chl *a* normalized TRIOS–FLH (mW m^{-2} $sr^{-1}\mu m^{-1}$per µg Chl *a* l^{-1}) against the Chl *a* concentration (µg l^{-1}). Multiple FLH measurements were taken at each station (per Chl *a* measurement). **b** Chl *a* normalized TRIOS–FLH (mW m^{-2} $sr^{-1}\mu m^{-1}$per µg Chl *a* l^{-1}) corrected for incident solar irradiation PAR against the Chl *a* concentration (µg l^{-1}). Extreme outliers (FLH/Chl *a* > 0.5) are left out of the figures

levels in the fluorescence image (Fig. 9b). Furthermore, MODIS–FLH data were plotted against MODIS-derived Chl *a* concentrations for the A transect, where relatively high values (max 0.03 mW m^{-2} sr^{-1} μm^{-1}) were measured (R^2 of 0.81, Fig. 10). In the B and C transects MODIS–FLH values were lower, sometimes even negative (no data shown).

Discussion

Phytoplankton fluorescence is widely regarded as a powerful tool for understanding phytoplankton biomass distribution and photosynthesis in the oceans (Falkowski and Kiefer 1985; Behrenfeld and Falkowski 1997). Phytoplankton biomass can nowadays be assessed through the use of airborne and spaceborne radiometers. High-resolution measurements in space and time of rates of photosynthesis are still in development, with passive and active fluorescence measurements as suitable candidate methods. Active fluorescence, most notably in the form of measurements of the photosynthetic efficiency (F_v/F_m), has been demonstrated as a useful in situ diagnostic for the physiological state (e.g. nutrient limitation) of phytoplankton (Boyd and Abraham 2001; Holeton et al. 2005; Behrenfeld et al. 2006). Alternatively, water-leaving, sun-induced fluorescence can be measured using remote sensing (shipboard or from space). In this study we explored the co-variance of photosynthetic efficiency, indicative of the physiological condition of the phytoplankton, and water-leaving fluorescence, thereby exploring the possibility of making more reliable remote-sensed estimates of primary production for true oceanic conditions in a similar way as was pioneered by Forster and Kromkamp (2004) for benthic microalgal mats.

The amount of useful measurements of water-leaving radiance taken during the KEOPS cruise was smaller than

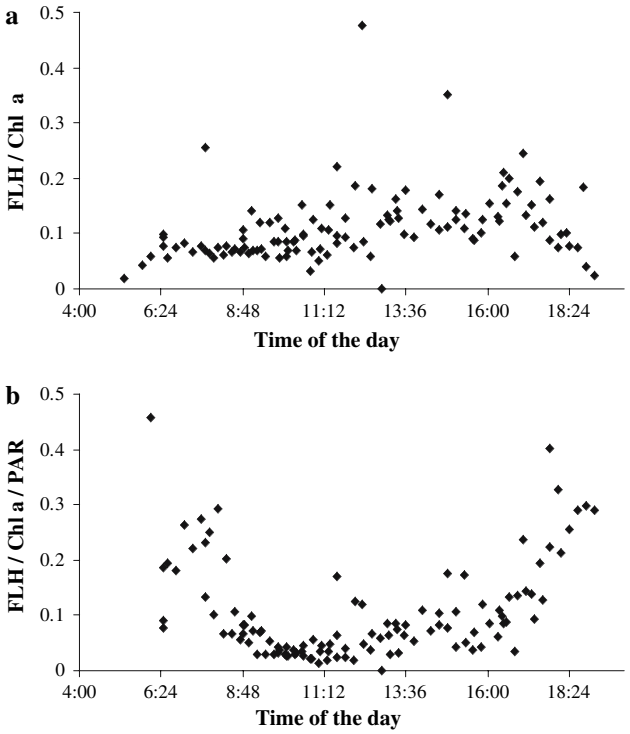

Fig. 8 **a** The TRIOS–FLH (mW m^{-2} sr^{-1} μm^{-1}) per unit Chl *a* (μg l^{-1}, 10 m depth) plotted against the time of the day at which the measurement was taken. **b** TRIOS–FLH (mW m^{-2} sr^{-1} μm^{-1}) per unit Chl *a* (μg l^{-1}, 10 m depth) normalized for the incident light intensity (PAR). Extreme outliers (FLH/Chl *a* >0.5, *y*-axis) are left out of the figures

we hoped. The wave activity was generally high, with as a result a lot of foam on the water surface. As foam is white, many water-leaving radiance spectra contained a high level of white reflectance that blurred the actual measurement. Selecting the spectra with the least reflectance left us with a limited dataset. And because the shipboard-sampled parameters (Chl *a*, F_0 and F_v/F_m) were often collected at nighttime or at dusk or dawn, a limited set of matches remained between the water-leaving fluorescence (TRIOS–FLH) and the discrete water samples. Cloudcover and mismatch between sampling times and satellite overpass further hampered the comparison between in situ measurements and MODIS satellite measurements. We therefore regarded the TRIOS sensors on board R.V. Marion Dufresne as satellite sensors mounted on board the ship, and focused on the co-variance between photosynthetic efficiency and water-leaving fluorescence, in relation to the sharp differences present in phytoplankton biomass and primary production in the Kerguelen research area.

Even for the shipboard fluorescence measurements, the signal was around the detection limit and since the detection limit or the signal to noise ratio were not exactly known, it was difficult to tell which measurements were valuable. This, in combination with the limited data set made it difficult to distinguish between the different biological and/or methodological factors that influenced the fluorescence measurements during the cruise. We did however observe clear differences in fluorescence parameters above the Plateau and at the open ocean: photosynthetic efficiency (F_v/F_m, Fig. 3a), as well as water-leaving fluorescence (TRIOS–FLH, Fig. 4a) were higher above the Plateau than at the open ocean. These differences reflected the higher Chl *a* concentrations (Fig. 1b) and the higher Chl *a* autofluorescence F_0 (Fig. 2) measurements. Especially the co-variance of active fluorescence measurements and sun-

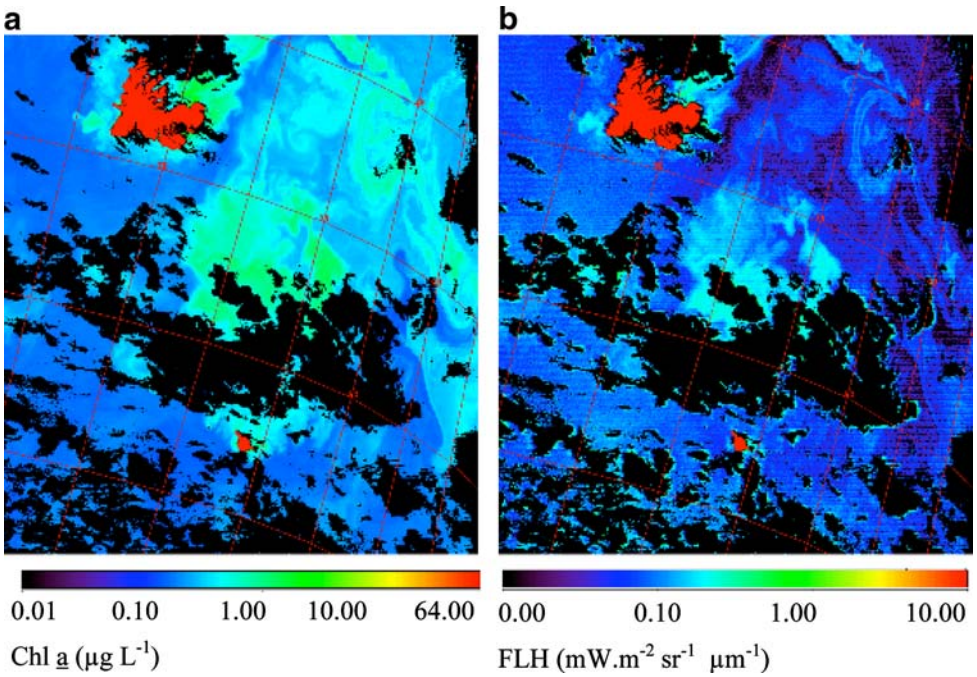

Fig. 9 MODIS images of **a** Chl *a* (μg l^{-1}) and **b** MODIS–FLH (mW.m^{-2} sr^{-1} μm^{-1}) on the 27th of January 2005. The Kerguelen Archipelago and the island Heard are coloured *red*, clouds are *black*. Mark the increased fluorescence at the edges of clouds, due to cloud reflectance

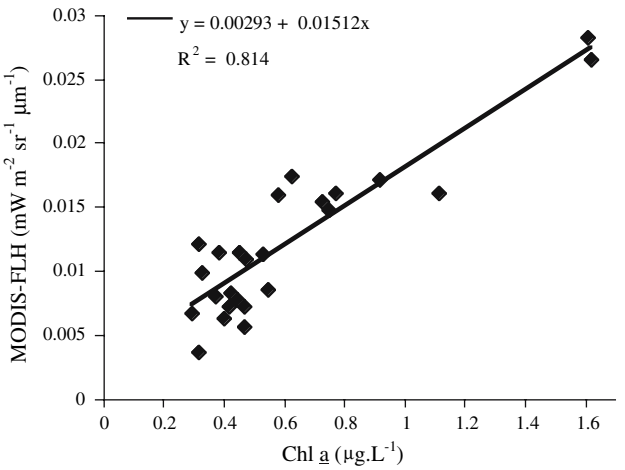

Fig. 10 Satellite MODIS–FLH (mW m^{-2} sr^{-1} μm^{-1}) against MODIS-derived Chl *a* concentrations (µg l^{-1}) for transect A

induced fluorescence is regarded as promising, because it opens up the way to extract information about the photosynthetic activity, hence primary production, from FLH measurements. A difference in fluorescence yield (TRIOS–FLH per unit Chl *a*), however, was not apparent from our data (Fig. 7a), not even when corrected for the amount of incident light (PAR) (Fig. 7b).

The observed mid-day depressions in both the fluorescence emitted by the sea surface (Fig. 8b) and the F_v/F_m (Fig. 3b) indicated that there were effects of non-photochemical quenching on both fluorescence properties. Mid-day depressions in fluorescence data (Falkowski and Kolber 1995) and F_v/F_m data (Boyd and Abraham 2001; Behrenfeld et al. 2006) have been reported before. The reduction in F_v/F_m at moderate to high (mid-day) irradiances is also a common phenomenon (Kromkamp and Forster 2003). In spite of the well-mixed surface waters during the KEOPS cruise, the decrease is most pronounced in the samples collected at 10 m depth (Fig. 3b). The fact that this mid-day depression in the maximum PSII efficiency was still visible after the dark adaptation (a standard procedure for the PHYTOPAM measurements), suggested that this decrease was not only due to rapid down regulation of photosynthesis caused by the xanthophyll cycle (Laney et al. 2005), but also by damage ("chronic down regulation") to PSII reaction centers. This down regulation during the day occurred on all sampling stations, and this process decreased the maximum differences in F_v/F_m between the open ocean and Plateau stations. Based on the diurnal variation in photosynthetic efficiency, the KEOPS area would fall into Behrenfeld et al.'s (2006) regime IV, polar waters with limited Fe supply and relative high macronutrient (nitrate) concentrations. The latter certainly was the case, especially at the open ocean, but above the Plateau low silicic acid concentrations (<2 µM) were reported (Mosseri et al. 2008). In Plateau surface water, the indigenous diatoms were still able to grow (Mosseri et al. 2008), in spite of silicic acid concentrations close to or below their half saturation values (Sarthou et al. 2005). Low silicic acid concentrations were sometimes reported to result in lower F_v/F_m values in *Thalassiosira weissflogii* (Lippemeier et al. 1999), sometimes reported to have no effects on F_v/F_m in small diatoms (Timmermans et al. 2008).

A relationship between the biomass-independent F_v/F_m parameter and the Chl *a* concentration was supposed to be absent. However, because the low F_v/F_m values in the open ocean stations strongly suggested Fe-limitation, the potential phytoplankton biomass, which could be developed was less than at the Plateau stations. There, the higher nutrient concentrations allowed a higher biomass and a clear relationship between the photosynthetic efficiency and Chl *a* concentration was observed. The pattern encountered matched well with the higher Fe availability in Plateau surface waters during the KEOPS cruise, most likely originating from the Plateau sediment (Blain et al. 2007), and a general better physiological state of the phytoplankton (Timmermans et al. 2008). Our findings also parallel those of Holeton et al. (2005), who reported a distinct increase in F_v/F_m, which they correlated with increased total dissolvable Fe concentrations originating from a benthic Fe source near South Georgia (Southern Ocean). The horizontal variation in biomass obtained by us using our various phytoplankton biomass proxies (Chl *a* concentrations, F_0) confirmed the distribution patterns of phytoplankton in the Kerguelen region observed microscopically by Armand et al. (2008) during the KEOPS cruise, including the general decline of the bloom.

Passive fluorescence (F_0) and shipboard TRIOS–FLH correlated well, explaining 77% of the variability (Fig. 6a). The remaining 23% of variability between F_0 and TRIOS–FLH was probably predominantly the result of the different nature of the light source by which the fluorescence signal was induced. The fluorescence emitted by the sea surface (TRIOS–FLH) was induced by natural solar radiation, whereas F_0 was induced by a very low light source of a continuous intensity generated by the PHYTOPAM instrument. However, also non-photochemical processes in the reaction centers of PSII could have caused variation in the correlation between F_0 and TRIOS–FLH. Similarly, the correlation between Chl *a* concentrations in the surface waters and shipboard TRIOS–FLH was strong, with an R^2 of 0.84 (Fig. 4a). The remaining variability of 16% could have several explanations. For example, during the KEOPS cruise a substantial shift in diatom species composition was observed at bloom stations over the Plateau. Armand et al. (2008), described a distinct change from a *Chaetoceros* bloom to a remnant *Eucampia antarctica* assemblage. The open ocean was dominated by *Fragilariopsis* species

throughout the whole cruise. There is not yet much known about the fluorescence properties (autofluorescence, photosynthetic efficiency as well as fluorescence yield) of different phytoplankton assemblages, but the species composition is expected to be one of the factors to have an effect on the amount of emitted fluorescence relative to the Chl *a* concentration. What these effects exactly are and how they interact with (changes in) environmental conditions should be further investigated.

The Chl *a* concentration calculated using the MODIS data indicated a decline at station A3 to levels of 0.45 μg l^{-1} in February (Fig. 5a). This was contradicted by the HPLC Chl *a* measurements that remained above the 1 μg l^{-1} level. An explanation for this discrepancy could be the change in specific absorbing properties of the phytoplankton. Underestimation of Chl *a* concentrations in Polar regions by the globally used satellite algorithms such as the OC3 algorithm (used for this paper) has been commonly observed, and was mainly ascribed to the effects of cold water on pigment packaging (Stramska et al. 2003). Irrespective of the discrepancy in Chl *a* concentrations from MODIS calculation and HPLC measurement, also the F_v/F_m measurements indicated a decline towards the end of the KEOPS cruise (Fig. 5b).

Our study, confirming earlier work by Stramska et al. (2003, 2006), has shown that the use of satellite-derived parameters in Polar regions, such as Chl *a* concentration and FLH can be questioned. Until a reliable Chl *a* algorithm for Polar regions is developed, it is probably inappropriate to use the standard Chl *a* parameters derived from satellite observations. During our research, a strong correlation between HPLC Chl *a* concentrations and the TRIOS–FLH measured at the sea surface was found. This correlation indicated that remotely sensed FLH could probably provide a better estimate of phytoplankton standing stock in Polar regions than the calculated Chl *a* concentrations from the blue–green ratio algorithms. Similar conclusions were drawn by Hu et al. (2005), who found that the FLH reflected the actual phytoplankton standing stock better than the Chl *a* concentration (MODIS, OC3M; SeaWiFS, OC4) in SW Florida coastal waters. However, the Chl *a* concentrations in the Southern Ocean are generally very low, with the exception of some bloom events, and probably too low to obtain reliable FLH measurements at most locations.

To our knowledge this is the first time that active and passive fluorescence measurements have been combined with water-leaving, sun-induced fluorescence measurements in the marine environment with natural phytoplankton in different physiological conditions. Most importantly, the PHYTOPAM-derived in situ F_0 and shipboard TRIOS–FLH matched reasonably well. In spite all of the complicating factors listed above, passive fluorescence F_0 and the fluorescence emitted by the sea surface clearly co-vary. The next step is to extract information about the photosynthetic efficiency from the FLH signal. Fluorescence yield, however, did not show significant differences in the research area. Most likely, this was due to the low signal and the diurnal variation in water-leaving fluorescence. Although, the presented results are encouraging, we need to do laboratory experiments to relate changes in photosynthetic efficiency, water-leaving fluorescence, and fluorescence yield, thereby enabling future establishment of the link between nutritional conditions and remote sensing properties such as MODIS fluorescence.

Acknowledgments The authors acknowledge Stephane Blain and Bernard Quéguiner (both at U. of Marseille, France) for making the KEOPS cruise possible. We thank captain Hedrich and his crew onboard RV Marion Dufresne for their professional support. Marcel Veldhuis (Royal NIOZ, Texel) was essential for collecting the TRIOS data on board, Corina Brussaard (Royal NIOZ, Texel) kindly prepared the Ocean Data View plot for Chl *a* (Fig. 1b), Jacco Kromkamp (NIOO CEME, Yerseke) provided many useful comments to a draft version of the manuscript and Claire Evans (Royal NIOZ, Texel) corrected the text. Our work would not have been possible without the logistic support of the French Polar Institute (IPEV, Institute Polaire Emile Victor, Brest). HvdW received an SRON grant EO-078. KRT received a travel and "Klein Vaarprogramma" grant from the Netherlands AntArctic Programme (ALW/NAAP).

References

Abbott MR, Letelier RM (1999) Algorithm theoretical basis document chlorophyll fluorescence (MODIS product number 20). NASA (http://www.modis.gsfc.nasa.gov/data/atbd)

Armand LK, Cornet-Barthaux V, Mosseri J, Quéguiner B (2008) Summer phytoplankton response on the Kerguelen Plateau during the KEOPS program: biomass and diversity. Deep Sea Res II, special KEOPS issue (in press)

Babin M, Morel A, Gentile B (1996) Remote sensing of sea surface sun-induced chlorophyll fluorescence: consequences of natural variations in the optical characteristics of phytoplankton and the quantum yield of chlorophyll fluorescence. Int J Remote Sens 17:2417–2448

Behrenfeld MJ, Falkowski PG (1997) Photosynthetic rates derived from satellite-based chlorophyll concentration. Limnol Oceanogr 42:1–20

Behrenfeld MJ, Kolber ZS (1999) Widespread iron limitation of phytoplankton in the South Pacific Ocean. Science 283:840–843

Behrenfeld MJ, Worthington K, Sherrell RM, Chavez FP, Strutton P, McPhaden M, Shea DM (2006) Controls of tropical Pacific Ocean productivity revealed through nutrient stress diagnostics. Nature 442:1025–1028

Blain S, Quéguiner B, Armand L, Belviso S, Bombled B, Bopp L, Bowie A, Brunet C, Brussaard C, Carlotti F, Christaki U, Corbière A, Durand I, Ebersbach F, Fuda J-L, Garcia N, Gerringa L, Griffiths B, Guigue C, Guillerm C, Jacquet S, Jeandel C, Laan P, Lefèvre D, Lomonaco C, Malits A, Mosseri J, Obernosterer I, Park Y-H, Picheral M, Pondaven P, Remenyi T, Sandroni V, Sarthou G, Savoye N, Scouarnec L, Souhaut M, Thuiller D, Timmermans K, Trull T, Uitz J, van-Beek P, Veldhuis M, Vincent D, Viollier E, Vong L, Wagener T (2007) Impacts of natural iron fertilisation on carbon sequestration in the Southern Ocean. Nature 446:1070–1074

Blain S, Sarthou G, Laan P (2008) Distribution of dissolved iron during the natural iron fertilisation experiments KEOPS (Kerguelen island, Southern Ocean). Deep Sea Res II, special KEOPS issue (in press)

Blain S, Tréguer P, Belviso S, Bucciarelli E, Denis M, Desabre S, Fiala M, Martin-Jézéquel V, Le Fèvre J, Myzaud P, Marty J-C, Razouls S (2001) A biogeochemical study of the island mass effect in the context of the iron hypothesis: Kerguelen Islands, Southern Ocean. Deep Sea Res I 48:163–187

Boyd PW, Abraham ER (2001) Iron mediated changes in phytoplankton photosynthetic competence during SOIREE. Deep Sea Res II 48:2529–2550

Bucciarelli E, Blain S, Tréguer P (2001) Iron and manganese in the wake of the Kerguelen Islands (Southern Ocean). Mar Chem 73:21–36

Chamberlin WS, Booth CR, Kiefer DA, Morrow JH, Murphy RC (1990) Evidence for a simple relationship between natural fluorescence, photosynthesis and chlorophyll in the sea. Deep Sea Res 37:951–973

De Baar HJW, De Jong JTM, Loscher BM, Veth C, Bathmann U, Smetacek V (1995) Importance of iron for plankton blooms and carbon dioxide drawdown in the Southern Ocean. Nature 373:412–415

Dierssen HM, Smith RC (2000) Bio-optical properties and remote sensing ocean color algorithms for Antarctic Peninsula waters. J Geophys Res 105:26301–26312

Falkowski PG, Kiefer DA (1985) Chlorophyll *a* fluorescence in phytoplankton: relationship to photosynthesis and biomass. J Plankt Res 7:715–731

Falkowski PG, Kolber Z (1995) Variations in chlorophyll fluorescence yields in phytoplankton in the worlds oceans. Austr J Plant Physiol 22:341–355

Forster RM, Kromkamp JC (2004) Modelling the effects of chlorophyll fluorescence from subsurface layers on photosynthetic efficiency measurements in microphytobenthic algae. Mar Ecol Prog Ser 284:9–22

Gower JFR (1980) Observations of in situ fluorescence of chlorophyll-a in Saanich inlet. Bound Layer Meteorol 18:235–245

Gower JFR, Brown L, Borstad GA (2004) Observations of chlorophyll fluorescence in west coast waters of Canada using the MODIS satellite sensor. Can J Remote Sens 20:1771–1786

Heuermann R, Reuter R, Willkomm R (1999) RAMSES: a modular multispectral radiometer for light measurements in the UV and VIS. Environ Sens Appl Proc 3821:279–285

Holeton CL, Nédélec F, Sanders R, Brown L, Moore CM, Stevens DP, Heywood KJ, Statham PJ, Lucas CH (2005) Physiological state of phytoplankton communities in the Southwest Atlantic sector of the Southern Ocean, as measured by fast repetition rate fluorometry. Polar Biol 29:44–52

Hu C, Muller-Karger FE, Taylor C, Carder KL, Kelble C, Johns E, Heil CA (2005) Red tide detection and tracing using MODIS fluorescence data: a regional example in SW Florida coastal waters. Remote Sens Environ 97:311–321

Huot Y, Brown CA, Cullen JJ (2005) New algorithms for MODIS sun-induced chlorophyll fluorescence and comparison with present data products. Limnol Oceanogr Methods 3:108–130

Kiefer DA, Chamberlin WS, Booth CR (1989) Natural fluorescence of chlorophyll a: relationship to photosynthesis and chlorophyll concentration in the western South Pacific gyre. Limnol Oceanogr 34:868–881

Kolber Z, Zehr J, Falkowski PG (1988) Effects of growth irradiance and nitrogen limitation on photosynthetic energy conversion in photosystem II. Plant Physiol 88:923–929

Kromkamp JC, Forster RM (2003) The use of variable fluorescence measurements in aquatic ecosystems: differences between multiple and single turnover measuring protocols and suggested terminology. Eur J Phycol 38:103–112

Laney SR, Letelier RM, Abbott MR (2005) Parameterizing the natural fluorescence kinetics of *Thalassiosira weissflogii*. Limnol Oceanogr 50:1499–1510

Letelier R, Abbott MR (1996) An analysis of chlorophyll fluorescence algorithms for the moderate resolution imaging spectrometer (MODIS). Remote Sens Environ 58:215–223

Lippemeier S, Hartig P, Colijn F (1999) Direct impact of silicate on the photosynthetic performance of the diatom *Thalassiosira weisflogii* assessed by on-and off-line PAM fluorescence measurements. J Plankt Res 2:269–283

Lorenzen J (1966) A method for the continuous measurement of in vivo chlorophyll concentration. Deep Sea Res 13:223–227

Martin JH, Fitzwater SE, Gordon RM (1990) Iron deficiency limits phytoplankton growth in Antarctic water. Glob Biogeochem Cycles 4:5–12

Mitchell BG (1992) Predictive bio-optical relationships for polar oceans and marginal ice zones. J Mar Syst 3:91–105

Mobley CD (1999) Estimation of the remote-sensing reflectance from above-surface measurements. Appl Opt 38:7442–7455

Mosseri J, Quéguiner B, Armand, Cornet-Barthaux V (2008) Impact of iron on silicon utilization by diatoms in the Southern Ocean: a case study of the Si/N cycle decoupling in a naturally iron-enriched area. Deep Sea Res II, special KEOPS issue (in press)

Neville RA, Gower JFR (1977) Passive remote sensing of phytoplankton via chlorophyll a fluorescence. J Geophys Res 82:3487–3493

O'Reilly JE, Maritorena S, Mitchell BG, Siegel DA, Carder KL, Garver S, Kahru M, McClain C (1998) Ocean color chlorophyll algorithms for SeaWiFS. J Geophys Res 103:24937–24953

Parsons TR, Maita Y, Lalli CM (1984) A manual of chemical and biological methods for seawater analysis. Pergamon, Oxford

Ras J, Claustre H, Uitz J (submitted) Spatial variability of phytoplankton pigment distributions in the Subtropical South Pacific Ocean: comparison between in situ and modelled data. Biogeosciences

Sarthou G, Timmermans KR, Blain S, Tréguer P (2005) Growth physiology and the fate of diatoms in the Ocean: a review. J Sea Res 53:25–42

Schreiber U, Neubauer C, Schliwa U (1993) PAM fluorometer based on medium-frequency pulsed Xe-flash measuring light: a highly sensitive new tool in basic and applied photosynthesis. Photosynth Res 36:65–72

Sedwick PN, DiTullio GR (1997) Regulation of algal blooms in Antarctic shelf waters by the release of iron from melting sea ice. Geophys Res Lett 24:2515–2518

Stramska M, Stramski D, Hapter R, Kaczmarek S, Ston J (2003) Bio-optical relationships and ocean color algorithms for the north polar region of the Atlantic. J Geophys Res 108:12–1–12–16

Stramska M, Stramski D, Kaczmarek S, Allison DB, Schwarz J (2006) Seasonal and regional differentiation of bio-optical properties within the north polar Atlantic. J Geophys Res 111:1–16

Timmermans KR, Veldhuis MJW, Laan P, Brussaard CPD (2008) Probing natural Fe fertilization near the Kerguelen (Southern Ocean) using natural phytoplankton assemblages and diatom cultures. Deep Sea Res II, special KEOPS issue (in press)

Van Heukelem L, Thomas CS (2001) Computer-assisted high-performance liquid chromatography method development with applications to the isolation and analysis of phytoplankton pigments. J Chromatom 910:31–49

Veldhuis MJW, Timmermans KR (2007) Phytoplankton dynamics during the EISENEX iron fertilisation experiment in the Southern Ocean: a comparative study of field and bottle incubation measurements. Aquat Micriobiol Ecol 47:191–208

Wernand MR (2002) Guidelines for (shipborne) auto-monitoring of coastal and ocean colour. Ocean Optics XVI Proceedings, Santa Fé